

Impedance characteristics of an active antenna at whistler mode frequencies

V. V. Paznukhov,¹ G. S. Sales,¹ K. Bibl,¹ B. W. Reinisch,¹ P. Song,¹ X. Huang,¹ and I. Galkin¹

Received 18 September 2009; revised 22 February 2010; accepted 23 March 2009; published 21 September 2010.

[1] We use the radio plasma imager (RPI) on the IMAGE satellite to investigate the impedance characteristics of an active electric antenna in space plasma at whistler mode frequencies. A dedicated experiment was carried out on 21–22 September 2005 for two orbits in the plasmasphere. The input impedance characteristics of the dipole antenna submerged in plasma is determined at whistler frequencies. The results are consistent with a physical model in which the antenna is negatively charged to a large voltage and the plasma around each antenna element forms an ion sheath that varies with time in its radius. Within the plasmasphere, these sheaths are a part of the antenna-plasma system and represent a capacitive component of the tuned antenna circuit. It is shown that, inside the plasmasphere, the RPI antenna capacitance varied from 430 to 480 pF. The plasma sheath formed around the antenna in the plasmasphere increases its capacitance by 20%–30% with respect to the near-free space capacitance (364 pF). Comparison of these values to model calculations shows good agreement with a difference smaller than 5%. Measurements of the antenna input resistance showed that, inside the plasmasphere, its value was between 200 and 500 Ω , varying considerably with changes in the ambient electron density and cyclotron frequency. The measured antenna input resistance is compared to model calculations.

Citation: Paznukhov, V. V., G. S. Sales, K. Bibl, B. W. Reinisch, P. Song, X. Huang, and I. Galkin (2010), Impedance characteristics of an active antenna at whistler mode frequencies, *J. Geophys. Res.*, 115, A09212, doi:10.1029/2009JA014889.

1. Introduction

[2] Recently, there has been a growing interest in placing radio wave transmitters on board Earth-orbiting satellites in order to study the Earth's magnetospheric environment. Transmitters operating in the very low frequency (VLF) band can potentially be used to modify the pitch angle distribution of energetic particles in the magnetosphere through wave-particle interaction [Lyons *et al.*, 1971, 1972; Abel and Thorne, 1998a, 1998b]. In order to achieve significant pitch angle diffusion of the radiation belt particles, a transmitter has to be able to radiate a high-power VLF wave. For designs of high-power spaceborne transmitters operating in a plasma environment, it is important to understand the interaction of the antenna at high voltages with the surrounding plasma. The radio plasma imager (RPI) instrument designed by the Center for Atmospheric Research of University of Massachusetts Lowell [Reinisch *et al.*, 2001, 2000] was used to study the high-voltage antenna interaction with the plasma in the whistler mode. RPI was designed for active sounding in the magnetosphere using frequencies covering the Earth's mag-

netospheric plasma resonances (3 kHz to 3 MHz). In 2004 and 2005, several experiments were carried out to assess the characteristics of the plasma sheath formed around the RPI antennas during whistler wave radiations. These efforts resulted in a better understanding of the antenna-plasma interaction and were important for the development of future space systems operating in this frequency range. In this paper, we present results of a dedicated experiment aimed at investigating the VLF antenna impedance characteristics in the magnetospheric plasma.

[3] For an active antenna in plasma at whistler frequencies, a substantial space charge sheath (dependent on the applied RF voltage) forms around the antenna elements, i.e., plasma in the vicinity of the antenna is not neutral. The formation of the sheaths is caused by the different responses of the electrons and ions to the changing antenna charge (voltage). In the whistler frequency range, the electrons respond to the changing electric field surrounding the antenna very quickly while the ions cannot move fast enough to follow the wave oscillations. The sheath properties vary rapidly with time as the antenna voltage and current oscillate during a wave cycle and also vary slowly with plasma conditions as the satellite travels in space. The presence of the plasma sheath affects the active antenna's electrical characteristics.

[4] A number of theoretical studies of radiation from a short dipole antenna surrounded by plasma have been

¹Center for Atmospheric Research, University of Massachusetts Lowell, Lowell, Massachusetts, USA.

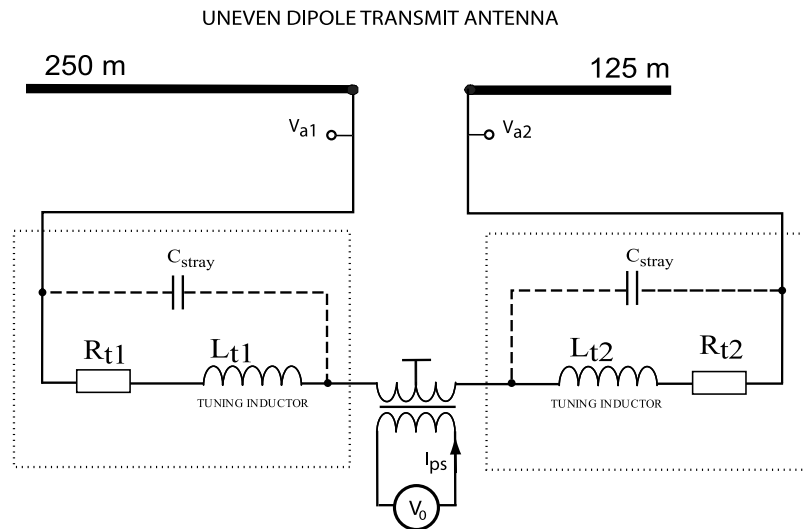


Figure 1. Schematic diagram of the RPI transmitting system. Elements L_{t1} and L_{t2} represent the “tuning inductors,” and R_{t1} and R_{t2} represent resistors. The voltages V_{a1} and V_{a2} were measured at the antenna terminals. The power supply voltage V_0 and current I_{ps} were measured in the primary circuit of the transformer.

carried out starting in the 1960s [e.g., *Mlodnosky and Garratt*, 1963; *Balmain*, 1964; *Despain*, 1966]. The subject was extensively studied in the 1970s [e.g., *Koons et al.*, 1970; *Shkarofsky*, 1972; *Kuehl*, 1974; *Laframboise et al.*, 1975; *Adachi et al.*, 1977], and work continued later on until recently [e.g., *James*, 2000; *Nikitin and Swenson*, 2001; *James*, 2003]. While these works have brought a conceptual understanding of the antenna-plasma interaction, some models often lacked self-consistency, since in most cases electrostatic conditions were assumed and the radiation resistance was not considered in the system. A new self-consistent model has recently been proposed by *Song et al.* [2007] and numerically investigated by *Tu et al.* [2008]. In the former work, an analytical solution for a time-dependent one-dimensional situation was presented while assuming immobile ions. The latter work reported the results from a full-particle simulation code.

[5] Experimental investigations, however, were rare and were mainly made at the ionospheric heights. They were carried out on board the OV3-3 spacecraft [e.g., *Koons et al.*, 1970], ISIS satellite [*James*, 1980], and also rockets [*Chugunov et al.*, 2003; *James*, 2003]. In most cases, the measured voltage or antenna potential as function of operating frequency was compared to those calculated using impedance theories for dipole antenna in plasma. It has been demonstrated that an agreement between the observations and theory was reasonably good when the sheath effect is taken into account [e.g., *Koons et al.*, 1970; *James*, 1980] and that the propagation near the resonance cone requires special treatment [*Chugunov et al.*, 2003]. *Song et al.* [2007] reported some preliminary experimental results obtained with the RPI-IMAGE instrument and compared the measurements with their sheath model. The differences between the modeled and measured sheath capacitance was about 20%. The reason for this relatively large difference is likely because of the fact that some information used in the analysis was not directly obtained from the measurements but derived from the RPI engineering unit under various assumptions. In

order to eliminate this shortcoming, a new series of measurements was designed maximizing the capabilities of the RPI system. This experiment, which was given the name “V71,” in accordance with the internal RPI programming convention, was carried out in September 2005.

2. RPI Antenna-in-Plasma Tuning Experiment

2.1. Experiment Setup

[6] The IMAGE satellite [*Burch et al.*, 2001], launched in March 2000, was the first NASA mission dedicated to remote imaging of Earth’s magnetosphere. The satellite was on a polar orbit with an apogee of ~ 7.5 Re, perigee of < 1000 km, and an orbit period of 14.5 h. Among the imaging instruments on board the satellite was the radio plasma imager tasked to characterize the magnetospheric plasma using the radio frequency sounding technique. The RPI instrument consisted of an electronics unit, two 500 m tip-to-tip wire dipole antennas in the spin plane (referred to as x and y antennas), and a 20 m dipole along the spin z axis [*Reinisch et al.*, 2000]. RPI transmitted and received coded pulse signals in the frequency range from 3 kHz to 3 MHz. The long wire antennas were connected to the transmitter through “tuners” consisting of a set of inductors and capacitors. The tuner inductances and operating frequency could be adjusted in order to match the reactance of the RPI output circuit to the reactance of the antenna-plasma system. When the match occurred or the circuit was in tune, maximum power was delivered to the antenna system, monitored by the measurements of the voltages at the antenna and the current in the power supply. Figure 1 is a basic schematic diagram of the RPI sounder, which includes a separate tuner for each element of the dipole antenna. The resulting voltages on the antenna branches are opposite in phase.

[7] In the V71 experiment, RMS voltages were measured at the two input terminals of the antenna, relative to the instrument ground, marked V_{a1} and V_{a2} in Figure 1. No AC

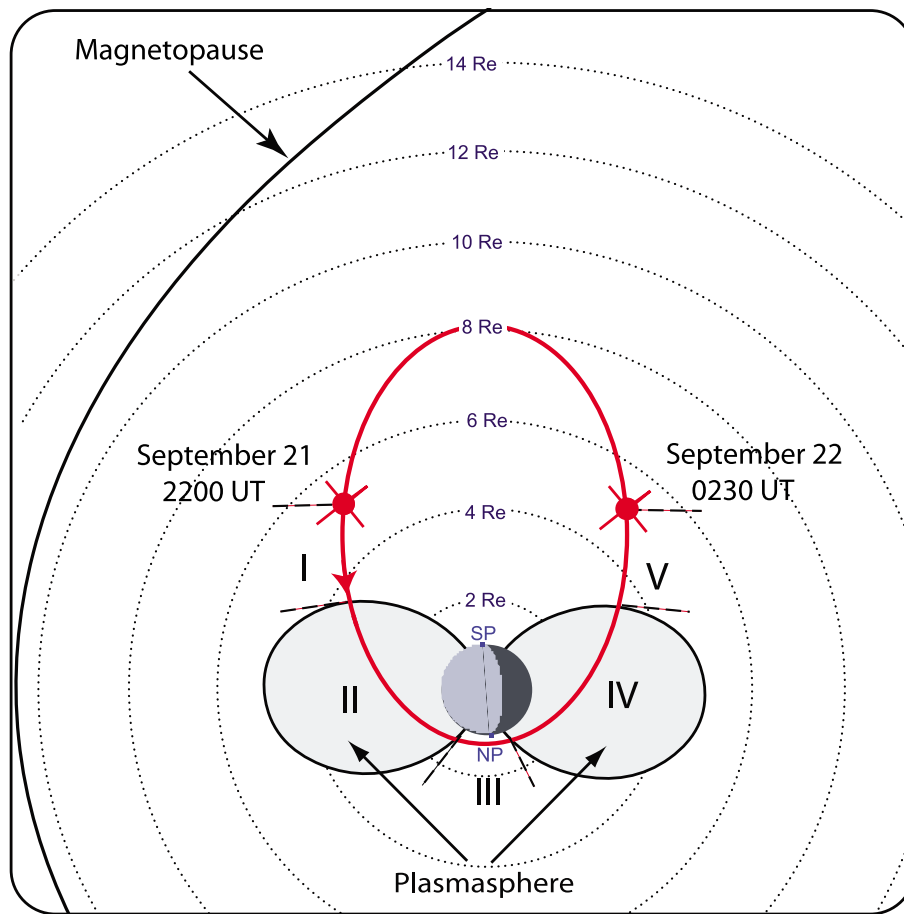


Figure 2. The RPI/IMAGE orbit for the V71 experiment. Labels I–V indicate the orbit regions listed in Table 1. Magnetopause is calculated from Tsyganenko 96 model (using Geopack software package), and plasmapause is approximately defined at $L = 5$.

currents in the antenna were measured, and the DC current measurements were made in the power supply.

[8] Only the x antenna was used for radiation in this experiment (the power supply in the y transmitter had failed early in the mission). By the time of this V71 experiment, one of the x antenna elements was shortened, likely by a meteorite impact. Resonance measurements had determined the length of the remaining section as 125 m. During the V71 experiment, only the voltage measurement at the shorter antenna element was quantitatively reliable.

[9] In the earlier experiment carried out in September 2004 and reported by *Song et al.* [2007], the range of the input impedance of the antenna-plasma system was unknown and the tuners were operated over a very large range of the inductances at the various frequencies, the combination of which resulted in a large range of tuning reactances. Using the knowledge of the range of the input impedance gained from the measurements made in 2004, the tuning algorithm in the V71 experiment was simplified by using a fixed inductor in each tuner. The RPI operating frequency was then stepped through a range of frequencies to find the best tuned frequency as indicated by a voltage maximum at the antenna input. The two tuning inductors selected for this experiment were 22.4 mH each. It was determined in the laboratory that

each inductor had a parallel stray capacitance of approximately 80 pF and a $\sim 50 \Omega$ internal resistance. In addition, there was a 100 Ω resistor connected in series with each tuning inductor. The frequency range covered by the V71 experiment was 18–80 kHz with 300 Hz steps and a dwell time on each frequency of ~ 0.125 s. For each frequency, the radiation lasted for more than 2000 cycles. If the antenna charging took few wave cycles as shown by *Tu et al.* [2008], the radiation can be considered steady state transmission. The RMS voltage was calculated by averaging RF samples for each frequency once every 3 min. Each V71 frequency scan was followed by a routine sounding measurement, from which the plasma frequency and electron gyrofrequency were derived; this program was repeated every 3 min.

[10] The data from two passes of the satellite were very similar, and the first pass from 2200 UT on 21 September 2005 to 0230 UT on 22 September 2005 is presented in this paper. During this pass, the measurements began in the outer magnetosphere before IMAGE entered the dayside plasmasphere; the measurements continued in the plasmasphere, over the southern polar cap region, and finally into the nightside plasmasphere as illustrated in Figure 2. The approximate plasmaspheric boundary in the figure is at $L = 5$. The observations can be divided into five nominal regions,

Table 1. IMAGE/RPI Orbit Regions During the V71 Experiment

Regions	Description	Time Interval (Approx.)
I	Outside the plasmasphere	2200 UT–2250 UT
II	Plasmasphere (on the dayside)	2250 UT–0010 UT
III	Polar cap region	0010 UT–0040 UT
IV	Plasmasphere (on the nightside)	0040 UT–0148 UT
V	Outside the plasmasphere	0145 UT–0230 UT

according to the satellite positions as shown in Figure 2. These regions are listed in Table 1.

[11] As part of its routine sounding program, RPI also measured the local plasma resonance frequencies such as the plasma frequency f_{pe} and electron-cyclotron frequency f_{ce} [Benson *et al.*, 2004; Galkin *et al.*, 2004]. These measurements, made 1.25 min after each sounding, are used to determine the local plasma parameters $X = f_{pe}^2/f_{res}^2$ and $Y = f_{ce}/f_{res}$ at each satellite position as plotted in Figure 3. These parameters are calculated using the resonance/tuned frequency f_{res} (the frequency at which the maximum antenna voltage was recorded), which is shown in Figure 4. Using the values of X and Y , the propagation modes in terms of the regions in the standard CMA diagram [Stix, 1962] are determined and marked in Figure 2. The portion of the orbit between 2320 UT (when $Y = 1$) and 0110 UT (when $Y = 1$ again), except for the time interval over the polar cap, represents whistler mode propagation region CMA 8 (i.e., $f_{res} \leq f_{ce} \leq f_{pe}$), which is of our primary interest in this work. For the periods with $X < 1$, i.e., before 2250 UT and after 0147 UT, the IMAGE satellite was in regions of very low electron densities outside the plasmasphere (CMA regions 1–3), and most of that time, the satellite was in CMA region 1, where plasma conditions can be approximated by the free space environment. This can also be seen from the fact that tuning frequency is almost constant outside the plasmasphere. Therefore, the antenna impedance in that part of the orbit can be approximated by that of free space environment.

2.2. Antenna Voltage Measurements

[12] The voltage measurements on the short antenna element are shown in Figure 4 as a function of sounding frequency and time, demonstrating the effects of the plasma environment on the antenna parameters.

[13] The tuned frequencies at which the maximum voltages occurred, i.e., the antenna-tuner resonance frequencies, are indicated in Figure 4 by a line with dots. As the satellite passed through the plasmasphere, significant changes in the tuned frequency are clearly visible, indicating changes in the antenna input impedance, resulted from the variations of the plasma sheath properties surrounding the antenna. As the IMAGE satellite entered the plasmasphere, the tuned frequency decreased quickly from 37.2 kHz (relatively constant in the low electron density region of the magnetosphere) to 34.3 kHz within the plasmasphere and then continued to decrease slowly to 33.0 kHz before entering the polar cap region. The tuned frequency variation on the other side of the plasmasphere was similar. This decrease in the tuned frequency within the plasmasphere corresponds to an increase in local electron density (i.e., the X parameter as seen in Figure 3) as the IMAGE satellite moved to lower altitudes near the perigee. In section 4, this variation is discussed in terms of the characteristics of the ion sheath that surrounds the antenna elements.

[14] Referring again to Figure 4, it is clear that the RPI system was well tuned (i.e., it shows a relatively sharp resonance and high voltage) in practically all regions, except the polar cap (CMA 7). The system was not tuned well (it exhibited the lowest maximum antenna voltage) at the times when the satellite was in the vicinity of $X = 1$ (around 2247 UT and 0145 UT), indicating a smaller Q factor, $Q = f_{res}/\Delta f$, where Δf is the half-power frequency width. Since the quality factor Q represents the ratio of the circuit reactance to its resistance, a lower Q factor indicates increased resistive loss in the system. It is likely that a portion of the system energy is

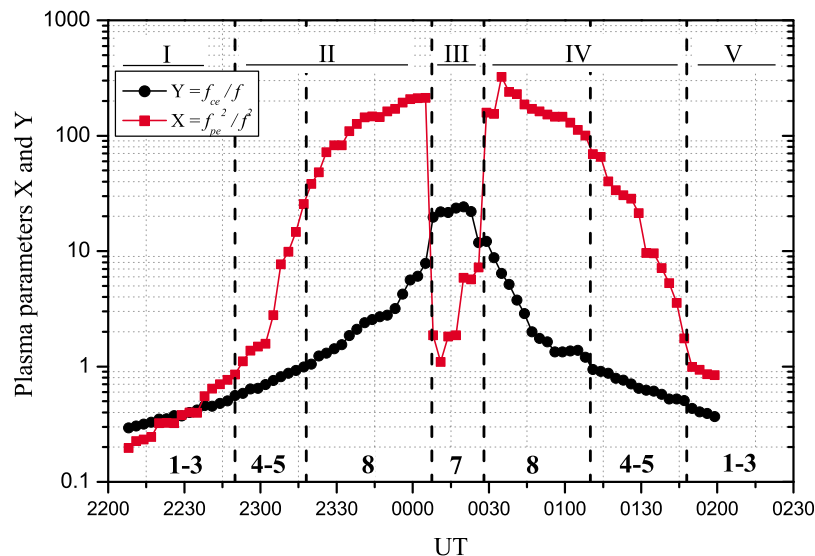


Figure 3. The plasma parameters X and Y during the V71 experiment. The values are determined for the RPI tuned frequency using the measured local plasma frequency and electron gyrofrequency. The Arabic numbers denote the regions in the standard CMA diagram. The orbit regions defined in Table 1 are indicated on top with Roman numbers.

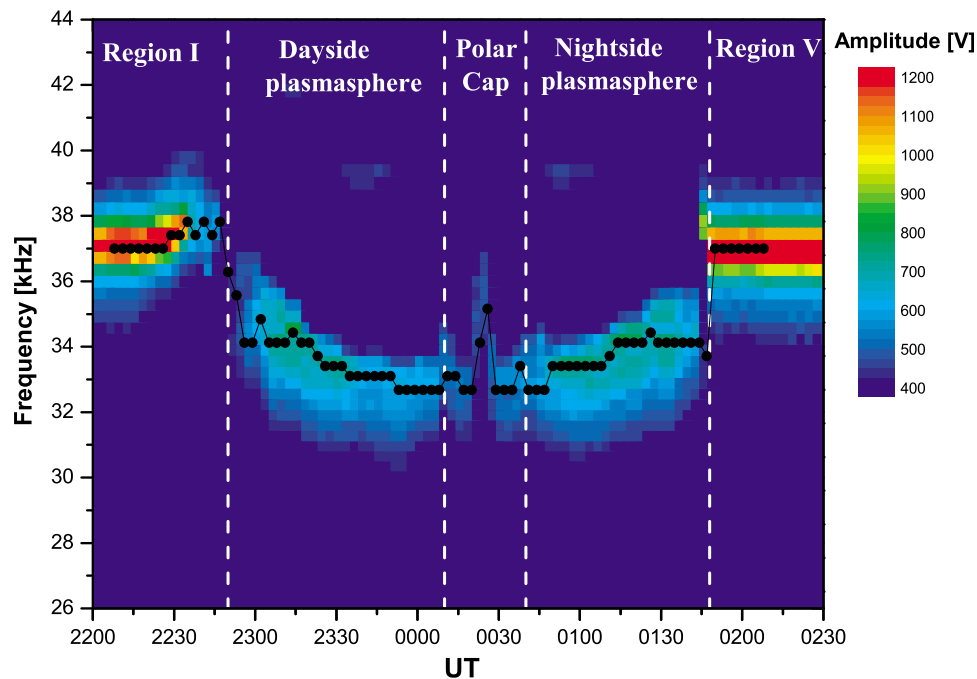


Figure 4. The measured antenna voltages as a function of time and frequency during the V71 experiment carried out on 21–22 September 2005. The RPI transmitting system was stepped in frequency at 300 Hz intervals. The line with dots indicates the frequency of the maximum voltage, i.e., resonance (or tuned) frequency. The five orbit regions listed in Table 1 are labeled.

lost to the local particle resonance absorption of the waves under this condition. In the low electron density regions outside the plasmasphere, the system was tuned very well (very narrow resonance with very high voltages or Q). In the whistler mode regions, inside the plasmasphere, the resonance was relatively sharp, but the maximum voltage was smaller compared to that outside the plasmasphere.

[15] In section 3, the two main characteristics of the RPI transmitting system are derived: the antenna input resistance and reactance. These two parameters were determined using the measured resonance (tuned) frequencies and the antenna voltages at the resonance frequency.

3. Antenna Impedance Measurements

3.1. Model and Approach

[16] *Song et al.* [2007] analyzed the structure of the ion sheaths surrounding dipole antenna elements in the plasmasphere and proposed a model for antenna-sheath interaction. In the model, it is assumed that the bare antenna in plasma is charged negatively to almost the maximum AC voltage on the antenna. As the plasma moves toward the antenna, the negatively charged antenna slows the electrons and accelerates ions so that the net currents generated by the two species cancels out, as required by steady state transmission. The antenna charge results from the depletion of the electrons surrounding the antenna and produces an ion sheath in this region. As the voltage of each antenna branch oscillates, the radius of the sheath varies. The sheath radius goes to zero at the maximum of the AC voltage and becomes largest when the voltage is at its minimum. *Tu et al.* [2008] presented a full-particle simulation of these processes. They confirmed the basic ideas of the model and further showed that the antenna

charging process takes only less than a wave cycle. They also investigated the effects of the ion motion. The ion effect reduces the antenna charge by few percentages. At the peak of the antenna voltage, which goes slightly positive, there is a brief period of electron conduction current associated with the electrons moving to the antenna. A much weaker but continuous ion conduction current balances the electron current in order to maintain the current continuity condition.

[17] When considering two branches of the antenna, the sheaths on the two sides oscillate with 180° phase shift. Electrons from one sheath move to the other sheath and form a displacement current, and hence, the sheath is capacitive in nature. This displacement current is the eventual driver of the radiation. The sheath conduction current between the plasma and the antenna is only few percentages of the total current in the system. The antenna is assumed in the *Song et al.* [2007] model to be long relatively to the sheath radius (antenna branches were 125 and 250 m long, and the sheath radius was less than 10 m under the condition). The relationship between the capacitance of a cylindrical sheath C_a and sheath radius r_s was shown to be

$$C_a(t) = \frac{2\pi\epsilon_0 l}{\ln\left[\frac{r_s(t)}{r_a}\right] - \frac{1}{2}}, \quad (1)$$

and the sheath radius r_s is given as

$$r_s(t) = \left[r_a^2 - \frac{2\sigma_0 r_a}{eN_e} + \frac{I_a(t)}{\pi\omega e l N_e} \right]^{1/2}, \quad (2)$$

where ϵ_0 is the permittivity of free space, e is the electron charge, l is the length of the individual antenna elements, and

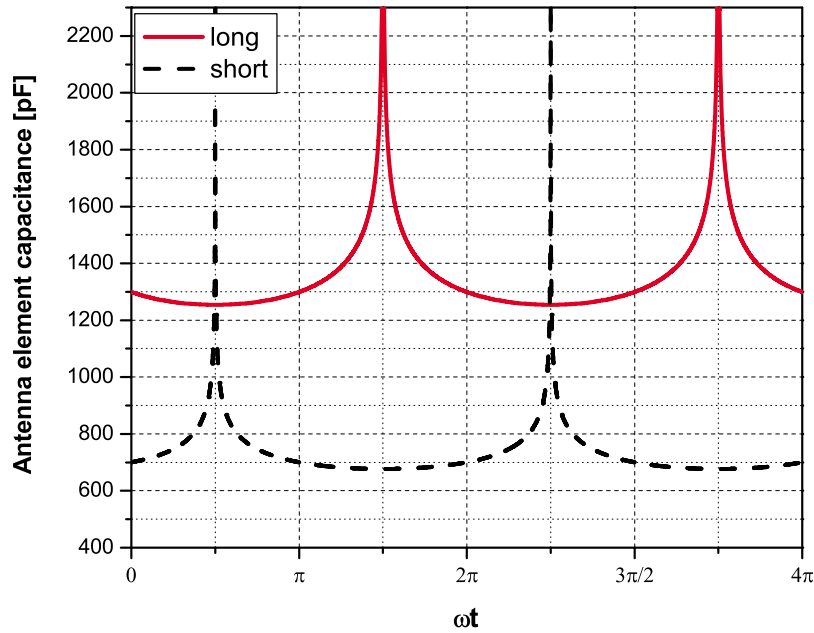


Figure 5. Calculated time variations of the RPI antenna element capacitances for typical plasmaspheric conditions. During 90% of time, the antenna-sheath capacitance is nearly constant, varying less than 5% from its average.

r_a is the radius of the antenna wire (0.0002 m for RPI), $\omega = 2\pi f$ is operating angular frequency, $I_a(t)$ is antenna current, σ_0 is DC antenna surface charge density, and N_e is the local electron density. The sheath capacitance is inversely proportional to the logarithm of the sheath radius. The variation in the size of the sheath is actually a dynamic process, and the sheath radius changes during the wave cycle, thus making antenna-sheath system, essentially, a nonlinear element. If antenna current varies with time as $\propto \sin \omega t$, then the sheath radius varies as $\propto \sqrt{\sin \omega t}$ (see equation (2)). Using equations (1)

and (2) and taking a typical value for the RPI antenna current of 200 mA and DC antenna surface charge density of $-1.7 \times 10^{-8} \text{ C cm}^{-2}$ [Tu et al., 2008], the RF time variations of the sheath capacitance for a wave cycle are calculated and the results are shown in Figure 5.

[18] During 90% of time in a cycle, the antenna-sheath capacitance is nearly constant, varying less than 5% from its average, with the spikes corresponding to the minimum sheath radius. The ratio of the capacitances is ~ 2 over most of the RF cycle, and the maximum of one sheath's capaci-

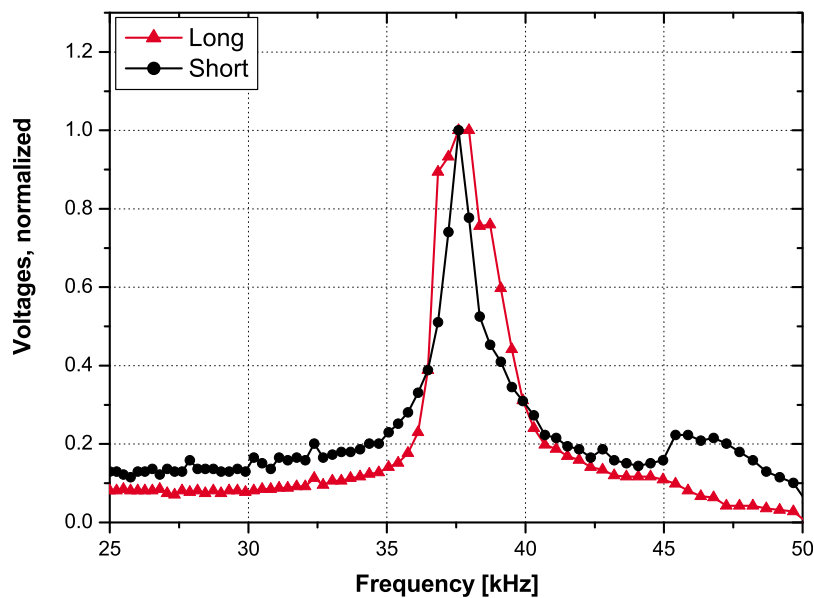


Figure 6. Normalized voltage measurements at the RPI antenna terminals. The main system resonance is observed at the same frequency at both antenna sides.

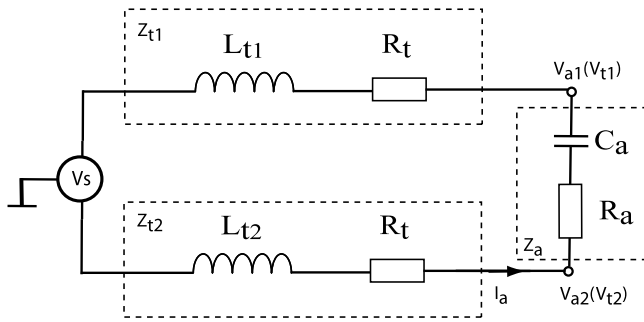


Figure 7. Simplified tuner-antenna-plasma circuit. Tuner elements L_{t1} , L_{t2} and R_{t1} , R_{t2} represent the original tuner elements modified by the parallel stray capacitances (see Figure 1) and the internal resistances of the inductors. V_s represents the source voltage in the secondary of the transformer. The antenna-plasma sheath system is represented by an input impedance Z_a with a capacitance C_a and resistance R_a .

tance corresponds to the minimum of the other. The minimum capacitance occurs when the sheath is at its maximum radius. Since the sheath capacitance does not vary significantly during an RF cycle, one can treat the variations as small perturbations around its average in the simplest approach, and therefore, a CW circuit analysis can be utilized. From the electric circuit point of view, the antenna-sheath system can be characterized by its effective impedance, which is nearly constant on the time scale of the RF cycle.

[19] Another very important question is whether the RPI antenna should be treated as a dipole or two individual monopoles. In principle, both situations are possible. However, in the V71 experiment, the dipole resonance was dominant, as seen from Figure 6, showing the measured

antenna voltages as function of frequency. As mentioned before, the voltage measurements on the longer antenna, V_{a1} , were made, but, unfortunately, the absolute values cannot be restored due to some system failure. This is why the normalized voltage values are shown in Figure 6. Clearly, the main resonance is observed at the same resonance frequency at both antenna halves, indicating that, in the first approach, the antenna can be regarded as an uneven dipole. Figure 7 shows an equivalent circuit, which is used to apply CW analysis.

3.2. Antenna Reactive Component

[20] The antenna-sheath system is now represented by the antenna capacitance C_a and antenna input resistance R_a . Elements L_t and R_t shown in Figure 1 represent the tuner inductors and resistors as modified by the effect of the parallel stray capacitance of ~ 80 pF and the internal resistance of the inductor of $\sim 50 \Omega$. The effect of the stray capacitance makes the effective inductance approximately 6% larger and is taken into account when calculating the tuner reactance. The voltage source V_s represents the voltage in the secondary circuit of the transformer shown in Figure 1. Although this voltage was not directly measured in the experiment, it is known that the source primary voltage V_o was at a relatively constant value of 20 V varying with the frequency by not more than $\pm 10\%$. Therefore, the secondary voltage V_s is assumed to be constant, independent of frequency.

[21] The antenna reactance is calculated from the RPI system resonance condition according to which a maximum voltage occurs when the capacitive antenna-sheath reactance equals the total inductive reactance of the two tuners, i.e., $\omega_{res}L_{t1} + \omega_{res}L_{t2} = 1/\omega_{res}C_a$ where ω_{res} is the angular resonant frequency for each frequency scan (as shown in Figure 4). Thus, it is straightforward to calculate the antenna capaci-

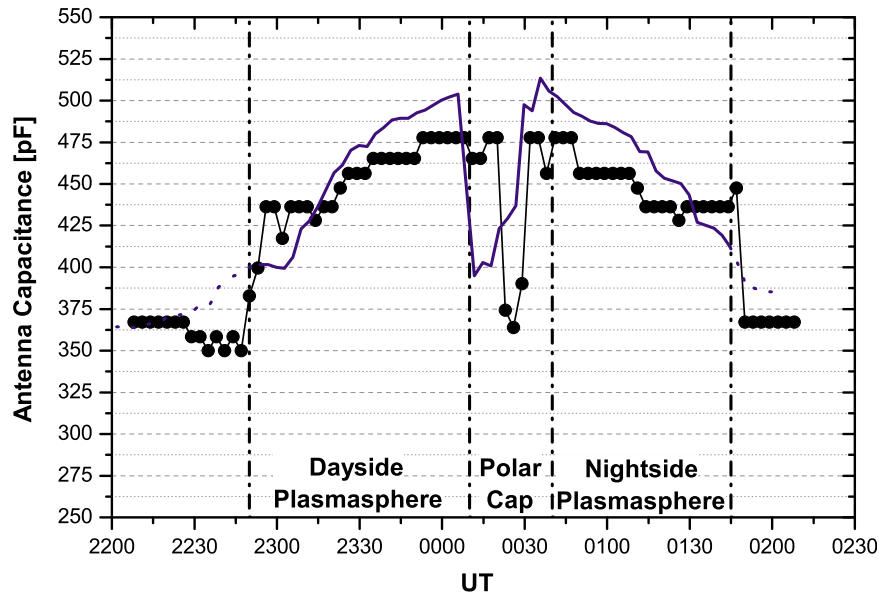


Figure 8. RPI antenna capacitance (dots) calculated using the known tuner inductances and the tuned (resonance) frequency yielding the maximum antenna voltage. Solid line shows the modeled RPI antenna capacitance [Song et al., 2007]. The dotted lines correspond to the regions outside the plasmasphere, in which the sheath model is not directly applicable.

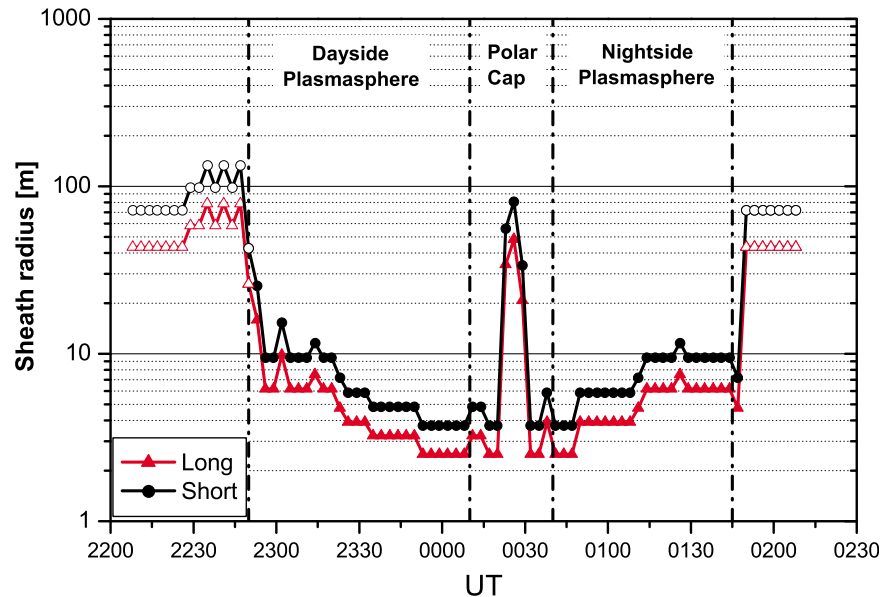


Figure 9. Variations of the effective radii of the RPI antenna sheaths during the V71 experiment. The open circles correspond to the regions outside the plasmasphere, in which the sheath model is not directly applicable.

tance $C_a = [\omega_{\text{res}}^2(L_{t1} + L_{t2})]^{-1}$. The calculated antenna capacitances are shown in Figure 8. Outside the plasmasphere, where the electron density was very low, the measured capacitance was 350–370 pF and can be interpreted as the dipole antenna capacitance in vacuum.

[22] Inside the plasmasphere, the antenna input capacitance varied from 430 to 480 pF. These variations are mainly associated with the plasma frequency variations. It is interesting to compare these results to model calculations. As shown above, the plasma sheath model proposed by *Song et al.* [2007] allows calculation of the antenna-sheath system capacitance in plasma. The results of the model calculation for the antenna-sheath capacitance for the conditions of the V71 experiment are shown in Figure 8 as a solid line. The local plasma densities (the main input to the model) were determined from the local RPI sounding resonance frequencies. Inside the plasmasphere, the difference between the experimental results and the model is generally less than 5%. There is a larger difference in the polar cap region, which is expected, because the model neglects the effects of the magnetic field. In the polar cap region, however, since f_{ce} is significantly greater than f_{pe} , the effect of magnetic field must be taken into account.

[23] The measured capacitance corresponds to the series of the antenna-sheath capacitances of the two unequal antenna elements. Unfortunately, from the available measurements, it is not possible to measure the capacitances and sheath characteristics separately for each antenna element. However, using equations (1) and (2) with the same antenna current through both elements, it is easy to see that for antenna lengths in a ratio of about 1:2, the ratio of corresponding capacitances is approximately 1:2 as well (as Figure 5 illustrates). Thus, the calculated total antenna capacitance can be split in two serial capacitances with the appropriate ratios. Then, using equation (1), it is straightforward to estimate the

averaged (over a wave cycle) sheath radius for each antenna element. Figure 9 shows the time variations of the radii of the antenna sheaths, which are determined from the calculated antenna capacitance. The radii varied from about 10 m as the satellite entered the plasmasphere to 3 m as the ambient plasma density increased until the satellite entered the polar cap region. Under the conditions of low electron densities found in the polar cap and outside the plasmasphere, the sheath model does not apply because the electron characteristic frequencies are less than the operating (tuned) frequency.

[24] In reality, of course, the sheath radius also varies within a wave cycle following the sinusoidal variation of RPI antenna voltage (as shown in section 3.1). However, since only the RMS voltages were measured during the V71 experiment, the derived antenna capacitances and sheath radii should be regarded as time averages over a wave cycle as assumed in *Song et al.*'s [2007] model. It is also worth mentioning that the harmonics associated with the square wave of the source signals of the RPI transmitter become insignificant when the system resonates at its fundamental frequency.

3.3. Antenna Input Resistance Measurement

[25] Determining the antenna input resistance is more complicated when compared to determining the antenna reactance, primarily because it is one order smaller than the reactance. The RMS voltage measurements on the short antenna were used for this purpose. As Figure 10 shows, inside the plasmasphere, the voltage measured on the short antenna element varied between 500 and 800 V.

[26] Referring to the equivalent circuit shown in Figure 7, since $V_a \gg V_s$ the measured antenna voltages are approximately equal to the voltages across the corresponding tuner elements (e.g., $V_{a1} \approx V_{t1}$, $V_{a2} \approx V_{t2}$). For the resonance

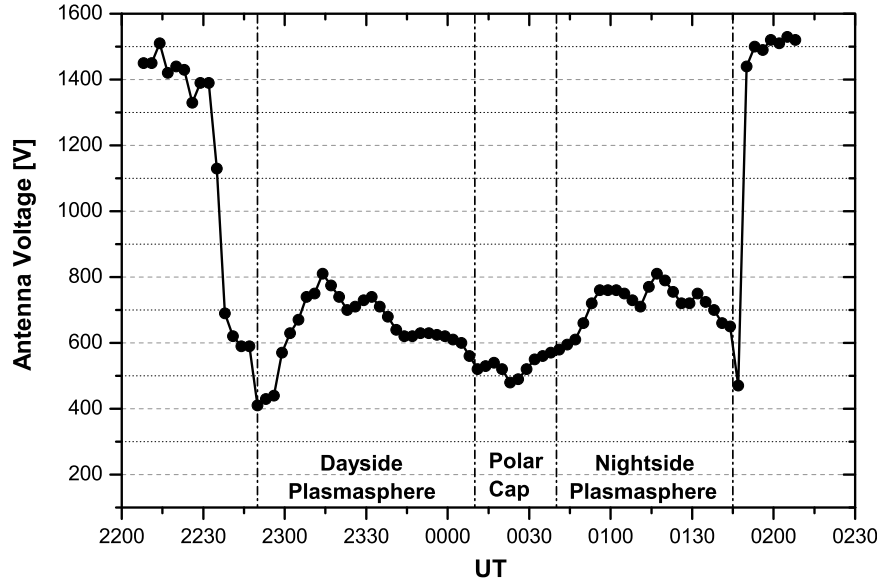


Figure 10. Measured RMS voltage on the short antenna element at the tuned (resonance) frequency. This voltage is used to calculate the antenna input resistance.

condition, the RMS voltage on tuner 2 (no phase measurements were made in the V71 experiment) can be written as

$$\begin{aligned}
 |V_{a2}| &= |I_a Z_{i2}| = \left| \frac{V_s}{Z_{t1} + Z_{i2} + Z_a} Z_{i2} \right| \\
 &= \left| \frac{V_s}{2R_t + j\omega L_{t1} + j\omega L_{i2} + R_a - j\frac{1}{\omega C_a}} Z_{i2} \right| \\
 &= \frac{|V_s|}{2R_t + R_a} |Z_{i2}|, \quad (3)
 \end{aligned}$$

where V_s is again the RMS source voltage in the secondary of the transformer.

[27] In principle, it is possible to determine the value of R_a from the above expression. However, since the voltage V_s in the secondary circuit of the transformer was not directly measured in V71 experiment (only the voltage V_o in the primary of the transformer was recorded), it is preferable to eliminate this term from the calculation by normalization. As mentioned above, the voltage in the transformer's primary V_o was practically constant with frequency and time; therefore, we assume that V_s was a constant as well. It is now possible to eliminate V_s from the calculation by comparing the measurements made at two different times, namely, outside and inside of the plasmasphere (orbit regions I, V and II, IV shown in Figure 2), which are denoted by superscripts *o* (outside) and *i* (inside). The voltages are then written as

$$|V_{a2}^o| = \frac{|V_s|}{2R_t + R_a^o} |Z_{i2}| \quad (4)$$

and

$$|V_{a2}^i| = \frac{|V_s|}{2R_t + R_a^i} |Z_{i2}|. \quad (5)$$

Note that outside the plasmasphere the plasma conditions corresponded to the propagation regions CMA 1–3 (see Figure 3). Since the resonance frequency was much greater than the local plasma frequency, these conditions were close to the “free space” conditions ($X \ll 1$). Under these conditions, the RPI antenna is effectively very short (the resonant wavelength is on the order of 10 km compared to the antenna length of 375 m), and therefore, the antenna resistance was assumed to be negligibly small in comparison to the tuner resistance, (i.e., $R_a^o \rightarrow 0$). Using this approximation, the antenna resistance $R_a^i(t)$ inside the plasmasphere is

$$R_a^i = 2R_t \left(\frac{|Z_{i2}^i|}{|Z_{i2}^o|} \frac{|V_{i2}^o|}{|V_{i2}^i|} - 1 \right). \quad (6)$$

Note that $|Z_{i2}| \equiv \sqrt{(\omega_{\text{res}} L_{i2})^2 + R_t^2} \approx \omega_{\text{res}} L_{i2}$, as $\omega_{\text{res}} L_{i2} \gg R_t$, and then

$$R_a^i = 2R_t \left(\frac{\omega_{\text{res}}^i |V_{i2}^o|}{\omega_{\text{res}}^o |V_{i2}^i|} - 1 \right), \quad (7)$$

where ω_{res}^o is the average tuned angular frequency outside the plasmasphere (relatively constant at 37.2 kHz) and ω_{res}^i is the time-varying tuned angular frequency inside the plasmasphere. The results for the antenna input resistance are shown in Figure 11. For times when IMAGE/RPI was inside the plasmasphere, the antenna input resistance varied considerably from 250 to 500 Ω . When the satellite was near the $X = 1$ point (at about 2245 UT), the input resistance was very large, indicating energy loss to the local plasma resonance. As the IMAGE satellite descended to lower altitudes into denser plasmas, the resistance increased steadily. Finally, in the polar cap region (around 0030 UT), the antenna input resistance increased to an even higher value on the order of 600 Ω .

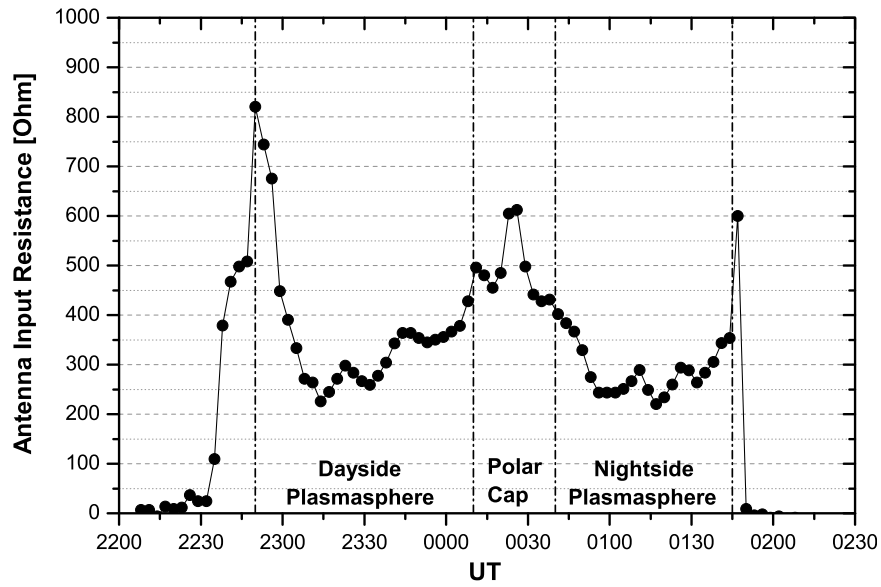


Figure 11. Calculated RPI antenna input resistance as a function of time during the V71 experiment.

3.4. Power Analysis

[28] Using the measurements made during the V71 experiment, it is possible to estimate the power dissipated by the entire system including losses in the antenna. The total power dissipated in the antenna-tuner system and the power dissipated by the antenna itself can be calculated as:

$$P_{tot} = |I_a|^2(R_a + 2R_t) = \left| \frac{V_{a2}}{Z_{t2}} \right|^2 (R_a + 2R_t) \quad (8)$$

$$P_a = \left| \frac{V_{a2}}{Z_{t2}} \right|^2 R_a. \quad (9)$$

The results of the calculations made using the above formulas are shown in Figure 12. The power dissipated in the high-density regions varies between 9 and 12 W, and outside the plasmasphere, it is about 20 W. The power dissipated by the antenna is shown in Figure 12 (bottom). Outside the plasmasphere, this power is essentially zero (since $R_a^o \rightarrow 0$), while inside the plasmasphere, it is a relatively constant value of about 5.3 W, with rather small time variations during the satellite passage through the plasmasphere. This relatively constant pattern seemed somewhat counterintuitive, as one might expect the power in the antenna to be positively cor-

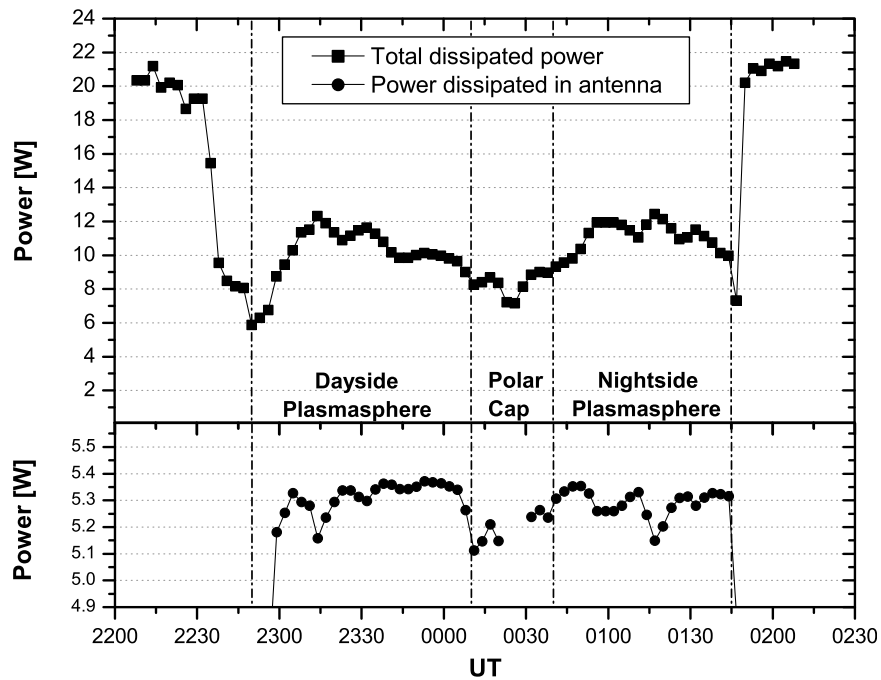


Figure 12. Total dissipated power and power dissipated by the RPI antenna system, calculated using equations (8) and (9) correspondingly. Outside the plasmasphere, the power dissipated by the antenna is essentially zero, since the antenna resistance is negligible.

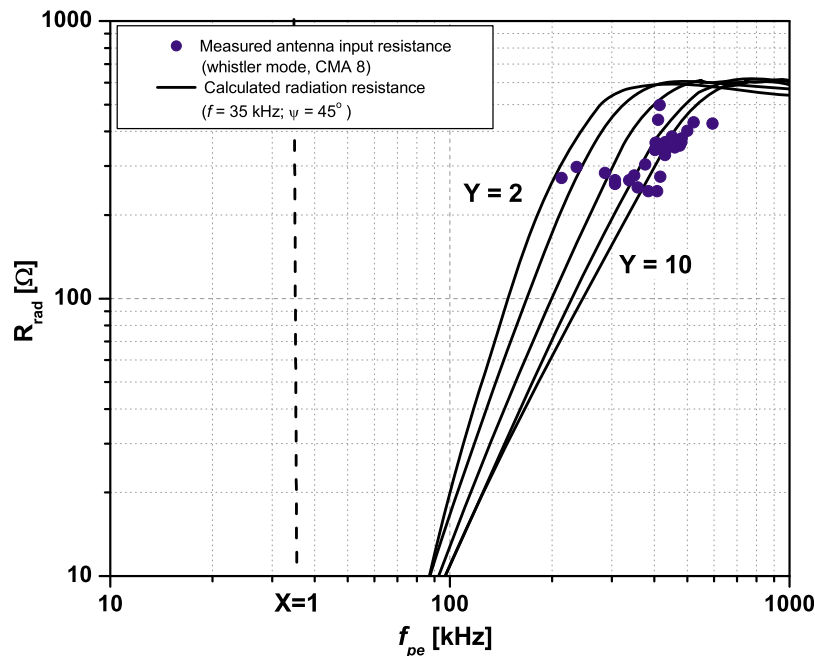


Figure 13. RPI antenna input resistances (dots) for the whistler mode frequencies (2320 UT–0110 UT) superposed on the theoretical radiation resistance [Song *et al.*, 2009] calculated for the X and Y values corresponding to the V71 experiment. The polar cap data points (0015 UT–0030 UT) are not included.

related with the total power dissipated in the system. This effect can be explained as follows. When the circuit is at the resonance, the antenna current is determined by the ratio of the source voltage (V_s) and the combined resistance of the tuner and antenna resistance ($2R_t + R_a$). Therefore, the antenna current is inversely related to the antenna resistance. In other words, the variations of the antenna current (as well as the total power dissipated in the system) are anticorrelated with the changes in antenna input resistance. Since the power dissipated in the antenna is a product of the square of antenna current and antenna resistance, the resulting function is relatively constant in time. We should point out that these results cannot distinguish the power lost in the antenna-plasma system from the radiation power.

4. Discussion and Summary

[29] Using the RPI-IMAGE satellite transmission system, a tuning experiment in the whistler frequency range was conducted, and an efficient system tuning was achieved. Despite the fact that the RPI instrument was not specifically designed for such an operation and a number of complications appeared in the experiment and data analysis, we have been able to determine the RPI antenna input impedance characteristics. Measurements of the RPI antenna reactance/capacitance have documented the effects of the ion sheath formation when the satellite was inside the plasmasphere with relatively high ambient electron densities. Our experimental data for the antenna capacitance is in good agreement with the theoretical calculations (see Figure 8) made using the model proposed by Song *et al.* [2007].

[30] The calculated antenna input resistance R_a varied significantly during the experiment. It was assumed that R_a was close to zero outside the plasmasphere in very low

electron density regions ($f \gg f_{pe}; f \gg f_{ce}$). This assumption of a small radiation resistance in the low-density regions is consistent with the well-known results for free space transmission [e.g., Balanis, 2005]. Inside the plasmasphere, at whistler frequencies ($f < f_{pe}; f < f_{ce}$) the antenna input resistance varies from 200 to 500 Ω . When the resonance frequency of the system was close to the local plasma frequency (i.e., $X = 1$), the antenna resistance increased to 600–800 Ω , indicating that the energy was absorbed by the electron plasma oscillations. The actual radiation resistance at whistler frequencies is crucial for potential space weather applications. A very important question is how much of the measured input antenna resistance is contributed to by the antenna radiation resistance and how much is dissipated locally near the antenna. Unfortunately, in our experiment, it is not possible to directly distinguish the losses near the antenna from those in the far field, i.e., from the radiation. However, there are indications that suggest that the major part of the measured antenna resistance represents the radiation resistance. First of all, it is not debatable that whistler frequency waves can be radiated in plasma, meaning that the sheath does not completely shield the antenna from the plasma. For example, Sonwalkar *et al.* [2007] reported RPI observations of whistler echoes reflected in the plasmasphere, suggesting a significant amount of whistler wave power radiated during the transmission. It is also possible to compare the RPI antenna input resistance measured in the V71 experiment with the theoretical values of the radiation resistance. A generalized theory for the radiated fields in plasma from a dipole antenna of arbitrary length has been presented in the work of Song *et al.* [2009]. Figure 13 shows the measured antenna input resistances (dots) together with the theoretically calculated radiation resistances in the range of the Y values (from 2 to about 10, see Figure 3) during the V71 experiment when the

whistler frequencies were transmitted. Within the whistler mode region (CMA 8), the agreement between experiment and theoretical calculations is very good. This suggests that, in the whistler mode region, a major part of the measured antenna input resistance in fact represents the antenna radiation resistance, and local losses are likely to be significantly smaller. The VLF power converted into the heating of the plasma, however, is capable to produce a radical change in the distribution of the local plasma around the antenna as has been shown by James [1980].

[31] An interesting fact is that RPI system was able to tune well over the entire experiment. At first, this appears surprising given the nonlinear dependence of the antenna sheath radius on the applied voltage (and therefore, the antenna capacitance), which varies during an RF cycle. The analysis given in section 3.1 provides an explanation, illustrating the fact that, on the time scale of the RF cycle, the antenna capacitance does not vary significantly (less than 5%) during the major part of the cycle, because of logarithmic dependence of the antenna capacitance on the sheath radius.

[32] Figures 8, 11, and 12 summarize the effect of the plasma sheath on the RPI antenna impedance and dissipated power at whistler mode frequencies. From Figure 8, it is evident that the effect of the plasma sheath on the antenna is to increase its capacitance by 20%–30% with respect to the free space capacitance of a dipole antenna. This is obvious when comparing the calculated capacitance values inside the plasmasphere to those in a region with very low density, close to vacuum (before 2215 UT). In contrast, the input resistance increases from essentially 0 to 700 Ω in the regions with high electron densities (see Figure 11). Finally, the total power dissipated by the system decreases by almost a factor of 2 as the satellite enters the plasmasphere (see Figure 12). Outside the plasmasphere (in near vacuum regions), practically all of the power is dissipated in the tuner system. However, inside the plasmasphere, about half of the total power is dissipated by the antenna, being converted into plasma losses and radiation.

[33] **Acknowledgment.** This research was supported by USAF grant FA8718-05-C-0070 of the AF Research Laboratory.

References

- Abel, B., and R. M. Thorne (1998a), Electron scattering loss in the Earth's inner magnetosphere: 1. Dominant physical processes, *J. Geophys. Res.*, *103*(A2), 2385–2396, doi:10.1029/97JA02919.
- Abel, B., and R. M. Thorne (1998b), Electron scattering loss in the Earth's inner magnetosphere: 2. Sensitivity to model parameters, *J. Geophys. Res.*, *103*(A2), 2397–2407, doi:10.1029/97JA02920.
- Adachi, S., T. Ishizone, and Y. Mushiaki (1977), Transmission line theory of antenna impedance in a magnetoplasma, *Radio Sci.*, *12*, 23–31.
- Balanis, C. A. (2005), *Antenna Theory: Analysis and Design*, 3rd ed., John Wiley & Sons, New York.
- Balmain, K. G. (1964), The impedance of a short dipole antenna in a magnetoplasma, *IEEE Trans. Antenn. Propag.*, *12*, 605–617.
- Benson, R. F., P. A. Webb, J. L. Green, L. Garcia, and B. W. Reinisch (2004), Magnetospheric electron densities inferred from upper-hybrid band emissions, *Geophys. Res. Lett.*, *31*, L20803, doi:10.1029/2004GL020847.
- Burch, J. L., et al. (2001), Views of Earth's magnetosphere with the IMAGE satellite, *Science*, *291*, 619–624.
- Chugunov, Y. V., E. A. Mareev, V. Fiala, and H. G. James (2003), Transmission of waves near the lower oblique resonance using dipoles in the ionosphere, *Radio Sci.*, *38*(2), 1022, doi:10.1029/2001RS002531.
- Despain, A. M. (1966), *Antenna impedance in the ionosphere*, Rep. 3, AFCRL-66-412, Upper Air Res. Lab., Univ. of Utah, Salt Lake City, Utah.
- Galkin, I., B. W. Reinisch, G. Grinstein, G. Khmyrov, A. Kozlov, X. Huang, and S. F. Fung (2004), Automated exploration of the radio plasma imager data, *J. Geophys. Res.*, *109*, A12210, doi:10.1029/2004JA010439.
- James, H. G. (1980), Tests of impedance theories for a transmitting dipole in an ionospheric plasma, *IEEE Trans. Antenn. Propag.*, *28*, 623–630.
- James, H. G. (2000), Electrostatic resonance-cone waves emitted by a dipole in the ionosphere, *IEEE Trans. Antenn. Propag.*, *48*, 1340–1348.
- James, H. G. (2003), Electromagnetic whistler mode radiation from a dipole in the ionosphere, *Radio Sci.*, *38*(1), 1009, doi:10.1029/2002RS002609.
- Koons, H. C., D. A. McPherson, and W. B. Harbridge (1970), Dependence of very-low-frequency electric field antenna impedance on magnetospheric plasma density, *J. Geophys. Res.*, *75*, 2490–2502.
- Kuehl, H. H. (1974), Electric field and potential near the plasma resonance cone, *Phys. Fluids*, *17*, 1275–1283.
- Laframboise, J. G., J. Rubinstein, and F. H. Palmer (1975), Theory of topside sounder transmission effects on antenna quasistatic sheath impedance, *Radio Sci.*, *10*, 773–784.
- Lyons, L. R., R. M. Thorne, and C. F. Kennel (1971), Electron pitch angle diffusion driven by oblique whistler mode turbulence, *J. Plasma Phys.*, *6*, 589–606.
- Lyons, L. R., R. M. Thorne, and C. F. Kennel (1972), Pitch-angle diffusion of radiation belt electrons within the plasmasphere, *J. Geophys. Res.*, *77*, 3455–3474.
- Mlodnosky, R. F., and O. K. Garriott (1963), The V.L.F. admittance of a dipole in the lower ionosphere, in *The Ionosphere, Proceedings of the International Conference*, edited by A. C. Stickland, pp. 484–491, Inst. Phys. and Physical Soc., London.
- Nikitin, P., and C. Swenson (2001), Impedance of a short dipole antenna in a cold plasma, *IEEE Trans. Antenn. Propag.*, *49*(10), 1377–1381.
- Reinisch, B. W., et al. (2000), The radio plasma imager investigation on the IMAGE spacecraft, *Space Sci. Rev.*, *91*, 319–359.
- Reinisch, B. W., et al. (2001), First results from the Radio Plasma Imager on IMAGE, *Geophys. Res. Lett.*, *28*(6), 1167–1170, doi:10.1029/2000GL012398.
- Shkarofsky, I. P. (1972), Nonlinear sheath admittance, currents, and charges associated with high peak voltage driven on a VLF/ELF dipole antenna moving in the ionosphere, *Radio Sci.*, *7*, 503.
- Song, P., B. W. Reinisch, V. Paznukhov, G. Sales, D. Cooke, J.-N. Tu, X. Huang, K. Bibl, and I. Galkin (2007), High-voltage antenna-plasma interaction in whistler wave transmission: Plasma sheath effects, *J. Geophys. Res.*, *112*, A03205, doi:10.1029/2006JA011683.
- Song, P., B. W. Reinisch, X. Huang, G. S. Sales, J. Tu, and V. V. Paznukhov (2009), Investigating stimulated wave-particle interaction of radiation belt particles with space-borne whistler mode transmitters, *Technical Report FA8718-05-C-0070*.
- Sonwalkar, V. S., A. Reddy, D. L. Carpenter, and B. W. Reinisch (2007), Observations of Magnetically Reflected (MR), Specularly Reflected (SR), and Back Scattered (BS) Whistler Mode (WM) Echoes Observed by Radio Plasma Imager (RPI) on IMAGE: Diagnostics of Electron Density, Density Structure, and Ion Composition, *American Geophysical Union, Fall Meeting 2007*, abstract #SM32A-04.
- Stix, T. H. (1962), *The Theory of Plasma Waves*, McGraw-Hill, New York.
- Tu, J., P. Song, and B. W. Reinisch (2008), Plasma sheath structures around a radio frequency antenna, *J. Geophys. Res.*, *113*, A07223, doi:10.1029/2008JA013097.
- K. Bibl, I. Galkin, X. Huang, V. V. Paznukhov, B. W. Reinisch, G. S. Sales, and P. Song, Center for Atmospheric Research, University of Massachusetts Lowell, Lowell, MA 01854, USA. (vadym_paznukhov@uml.edu)